Formation mechanisms of atmospheric nitrate and sulfate during the winter haze pollution periods in Beijing: gas-phase, heterogeneous and aqueous-phase chemistry

Pengfei Liu[1, 2, 3, 5], **Can Ye**[1, 3], **Chaoyang Xue**[1, 3], **Chenglong Zhang**[1, 2, 3], **Yujing Mu**[1, 2, 3, 4], **Xu Sun**[1, 6]

[1] Research Center for Eco-Environmental Sciences, Chinese Academy of Sciences, Beijing, 100085, China.
[2] Center for Excellence in Urban Atmospheric Environment, Institute of Urban Environment, Chinese Academy of Sciences, Xiamen, 361021, China.
[3] University of Chinese Academy of Sciences, Beijing, 100049, China.
[4] National Engineering Laboratory for VOCs Pollution Control Material & Technology, University of Chinese Academy of Sciences, Beijing, 100049, China.
[5] Key Laboratory of Atmospheric Chemistry, China Meteorological Administration, Beijing, 100081, China.
[6] Beijing Urban Ecosystem Research Station, Beijing, 100085, China.
Correspondence: Yujing Mu (yjmu@rcees.ac.cn)

Abstract

A vast area in China is currently going through severe haze episodes with drastically elevated concentrations of $PM_{2.5}$ in winter. Nitrate and sulfate are main constituents of $PM_{2.5}$ but their formations via NO_2 and SO_2 oxidation are still not comprehensively understood, especially under different pollution or atmospheric relative humidity (RH) conditions. To elucidate formation pathways of nitrate and sulfate in different polluted cases, hourly samples of $PM_{2.5}$ were collected continuously in Beijing during the wintertime of 2016. Three serious pollution cases were identified reasonably during the sampling period and the secondary formations of nitrate and sulfate were found to make a dominant contribution to atmospheric $PM_{2.5}$ under the relatively high RH condition. The significant correlation between NOR (NOR = NO_3^-/ (NO_3^-+NO_2)) and $[NO_2]^2 \times [O_3]$ during the nighttime under the RH≥60% condition indicated that the heterogeneous hydrolysis of N_2O_5 involving aerosol liquid water was responsible for the nocturnal formation of nitrate at the extremely high RH levels. The more coincident trend of NOR and [HONO] × [DR]

(direct radiation) × [NO_2] than [Dust] × [NO_2] during the daytime under the 30%<RH<60% condition provided convincing evidence that the gas-phase reaction of NO_2 with OH played a pivotal role in the diurnal formation of nitrate at moderate RH levels. The extremely high mean values of SOR (SOR = SO_4^{2-} / (SO_4^{2-}+SO_2)) during the whole day under the RH≥60% condition could be ascribed to the evident contribution of SO_2 aqueous-phase oxidation to the formation of sulfate during the severe pollution episodes. Based on the parameters measured in this study and the known sulfate production rate calculation method, the oxidation pathway of H_2O_2 rather than NO_2 was found to contribute greatly to the aqueous-phase formation of sulfate.

1. Introduction

In recent years, severe haze has occurred frequently in Beijing as well as the North China Plain (NCP) during the wintertime, which has aroused great attention from the public due to its adverse impact on atmospheric visibility, air quality and human health (Chan and Yao, 2008;Zhang et al., 2012;Zhang et al., 2015).

To mitigate the severe haze pollution situations, a series of regulatory measures for primary pollution sources have been implemented by the Chinese government. For example, coal combustion for heating in winter has gradually been replaced with electricity and natural gas in the NCP, coal-fired power plants have been strictly required to install flue-gas denitration and desulfurization systems (Chen et al., 2014), the stricter control measures such as terminating production in industries and construction as well as the odd and even number rule for vehicles have been performed in megacities during the period of the red alert for haze and so on. These actions have made tremendous effects to decline pollution levels of primary pollutants including $PM_{2.5}$ (fine particulate matter with an aerodynamic diameter less than 2.5 μm) in recent years (Li

et al., 2019). However, the serious pollution events still occurred in many areas of Beijing-Tianjin-Hebei (BTH) region in December 2016 and January 2017 (Li et al., 2019). It has been acknowledged that the severe haze pollution is mainly ascribed to stagnant meteorological conditions with high atmospheric relative humidity (RH) and low mixed boundary layer height, strong emissions of primary gaseous pollutants and rapid formation of secondary inorganic aerosols (SIAs, the sum of sulfate, nitrate and ammonium), especially sulfate and nitrate (Cheng et al., 2016;Guo et al., 2014;Huang et al., 2014). Some studies suggested that the contribution of SIAs to $PM_{2.5}$ was higher than 50% during the most serious haze days (Quan et al., 2014;Xu et al., 2017;Zheng et al., 2015a).

Generally, atmospheric sulfate and nitrate are formed through the oxidations of the precursor gases (SO_2 and NO_2) by oxidants (e.g. OH radical, O_3) via gas-phase, heterogeneous and aqueous-phase reactions (Ravishankara, 1997;Wang et al., 2013;Yang et al., 2015). It should be noted that the recent study proposed the remarkable emissions of primary sulfate from residential coal combustion with the sulfur contents of coal in range of 0.81-1.88% in Xi'an (Dai et al., 2019), but the primary emissions of sulfate could be neglected due to the extremely low sulfur content of coal (0.26-0.34%) used prevailingly in the NCP (Du et al., 2016;Li et al., 2016). Atmospheric RH is a key factor that facilitates the SIAs formation and aggravates the haze pollution (Wu et al., 2019), and hence the secondary formations of sulfate and nitrate are simply considered to be mainly via gas-phase reaction at relatively low atmospheric RH levels (RH<30%) and heterogeneous reactions and aqueous-phase reactions at relatively high atmospheric RH levels (RH>60%) (Li et al., 2017). However, their formation mechanisms at different atmospheric RH levels still remain controversial and unclear (Cheng et al., 2016;Ge et al., 2017;Guo et al., 2017;Li

et al., 2018;Liu et al., 2017a;Wang et al., 2016;Yang et al., 2017). For example, the recent studies proposed that atmospheric SO_2 oxidation by NO_2 dissolved in aqueous aerosol phases under the extremely high atmospheric RH conditions played a dominant role in sulfate formation under almost neutral aerosol solutions (a pH range of 5.4-7.0) during the serious pollution periods (Cheng et al., 2016;Wang et al., 2018a;Wang et al., 2016). However, Liu et al. (2017a) and Guo et al. (2017) found that the aerosol pH estimated by ISORROPIA-II model was moderately acidic (a pH range of 3.0-4.9) and thus the pathway of SO_2 aqueous-phase oxidation by dissolved NO_2 was unimportant during severe haze events in China. Additionally, although the pathway of N_2O_5 heterogeneous hydrolysis has been recognized as being responsible for the nocturnal formation of NO_3^- under relatively high atmospheric RH conditions (Tham et al., 2018;Wang et al., 2018b;Wang et al., 2018c), the effects of NO_2 gas-phase chemistry and NO_2 heterogeneous chemistry on the diurnal formation of NO_3^- under moderate atmospheric RH conditions (30%<RH<60%) have not yet been understood. Therefore, measurements of the species in $PM_{2.5}$ in different polluted cases during the wintertime are urgently needed to elucidate formation pathways of sulfate and nitrate.

In this study, hourly filter samples of $PM_{2.5}$ were collected continuously in Beijing during the wintertime of 2016, and the pollution characteristics and formation mechanisms of sulfate and nitrate in the $PM_{2.5}$ samples were investigated comprehensively under different atmospheric RH conditions in relation to gas-phase, heterogeneous and aqueous-phase chemistry.

2. Materials and Methods

2.1. Sampling and analysis

The sampling site was chosen on the rooftop (around 25 m above the ground) of a six-story

building in Research Center for Eco-Environmental Sciences, Chinese Academy of Sciences (RCEES, CAS), which was located in the northwest of Beijing and had been described in detail by our previous studies (Liu et al., 2016;Liu et al., 2017b). The location of the sampling site (40°00′29.85″ N, 116°20′29.71″ E) is presented in Figure S1. Hourly $PM_{2.5}$ samples were collected on prebaked quartz fiber filters (90mm, Munktell) from January 7th to 23th of 2016 by median-volume samplers (Laoying-2030) with a flow rate of 100 L min^{-1}. Water-soluble ions (WSI), including Na^+, NH_4^+, Mg^{2+}, Ca^{2+}, K^+, Cl^-, NO_2^-, NO_3^- and SO_4^{2-}, as well as carbon components including organic carbon (OC) and element carbon (EC) in the filter samples were analyzed by ion chromatography (Wayeal IC6200) and thermal optical carbon analyzer (DRI-2001A), respectively (Liu et al., 2017b). Analysis relevant for quality assurance & quality control (QA/QC) was presented in detail in section M1 of the Supplementary Information (SIs). Atmospheric H_2O_2 and HONO were monitored by AL2021-H_2O_2 monitor (AERO laser, Germany) and a set of double-wall glass stripping coil sampler coupled with ion chromatography (SC-IC), respectively (Ye et al., 2018;Xue et al., 2019a;Xue et al., 2019b). More details about the measurements of H_2O_2 and HONO were ascribed in section M2 of the SIs. Meteorological data, including wind speed, wind direction, ambient temperature and RH, as well as air quality index (AQI) derived by $PM_{2.5}$, SO_2, NO_x, CO and O_3 were obtained from Beijing urban ecosystem research station in RCEES, CAS (http://www.bjurban.rcees.cas.cn/).

2.2. Aerosol liquid water contents and pH prediction by ISORROPIA-II model

The ISORROPIA-II model was employed to calculate the equilibrium composition for Na^+-K^+-Ca^{2+}-Mg^{2+}-NH_4^+-Cl^--NO_3^--SO_4^{2-}-H_2O aerosol system, which is widely used in regional and global atmospheric models and has been successfully applied in numerous studies for

predicting the physical state and composition of atmospheric inorganic aerosols (Fountoukis and Nenes, 2007;Guo et al., 2015;Shi et al., 2017). It can be used in two modes: forward mode and reverse mode. Forward mode calculates the equilibrium partitioning given the total concentrations of gas and aerosol species, whereas reverse mode involves predicting the thermodynamic compositions based only on the concentrations of aerosol components. Forward mode was adopted in this study because reverse mode calculations have been verified to be not suitable to characterize aerosol acidity (Guo et al., 2015;Hennigan et al., 2015;Murphy et al., 2017;Pathak et al., 2004;Weber et al., 2016). The ISORROPIA-II model is available in "metastable" or "solid + liquid" state solutions. Considering the relatively high RH during the sampling period, the metastable state solution was selected in this study due to its better performance than the latter (Bougiatioti et al., 2016;Guo et al., 2015;Liu et al., 2017a;Weber et al., 2016). Additionally, although the gaseous HNO_3, H_2SO_4, HCl and NH_3 were not measured in this study, gas-phase input with the exception of NH_3 has an insignificant impact on the aerosol liquid water contents (ALWC) and pH calculation due to the lower concentrations of HNO_3, H_2SO_4 and HCl than NH_3 in the atmosphere (Ding et al., 2019;Guo et al., 2017). Based on the long-term measurement in the winter of Beijing, an empirical equation between NO_x and NH_3 concentrations was derived from the previous study (Meng et al., 2011), that is, $NH_3\,(ppb) = 0.34 \times NO_x\,(ppb) + 0.63$, which was employed for estimating the NH_3 concentration in this study. The predicted daily average concentrations of NH_3 varied from 3.3 μg m^{-3} to 36.9 μg m^{-3}, with a mean value of 16.6 μg m^{-3} and a median value of 14.6 μg m^{-3}, which were in line with those (7.6-38.1 μg m^{-3}, 18.2 μg m^{-3} and 16.2 μg m^{-3} for the daily average concentrations, the mean value and the median value of NH_3, respectively) during the winter of 2013 in Beijing in the previous study (Zhao et al., 2016).

Then, the aerosol pH could be calculated by the following equation:

$$pH = -log_{10}\frac{1000\times H^+}{W}$$

where H^+ (μg m^{-3}) and W (μg m^{-3}) are the equilibrium particle hydrogen ion concentration and aerosol water contents, respectively, both of which could be output from ISORROPIA-II.

2.3. Production of sulfate in aqueous-phase reactions

The previous studies showed that there were six pathways of the aqueous-phase oxidation of SO_2 to the production of sulfate, i.e. H_2O_2 oxidation, O_3 oxidation, NO_2 oxidation, transition metal ions (TMI) + O_2 oxidation, methyl hydrogen peroxide (MHP) oxidation and peroxyacetic acid (PAA) oxidation (Cheng et al., 2016;Zheng et al., 2015a). Because some TMIs, such as Ti(III), V(III), Cr(III), Co(II), Ni(II), Cu(II) and Zn(II), displayed much less catalytic activities (Cheng et al., 2016), only Fe(III) and Mn(II) were considered in this study. In addition, due to the extremely low concentrations of MHP and PAA in the atmosphere, their contributions to the production of sulfate could be ignored (Zheng et al., 2015a). To investigate the formation mechanism of sulfate during the serious pollution episodes, the contributions of O_3, H_2O_2, NO_2 and Fe(III) + Mn(II) to the production of sulfate in aqueous-phase reactions were calculated by the formulas as follows (Cheng et al., 2016;Ibusuki and Takeuchi, 1987;Seinfeld and Pandis, 2006):

$$-(\frac{d[S(IV)]}{dt})_{O_3} = (k_0[SO_2\cdot H_2O] + k_1[HSO_3^-] + k_2[SO_3^{2-}])[O_{3(aq)}] \quad \text{(R1)}$$

$$-(\frac{d[S(IV)]}{dt})_{H_2O_2} = \frac{k_3[H^+][HSO_3^-][H_2O_{2(aq)}]}{1+K[H^+]} \quad \text{(R2)}$$

$$-(\frac{d[S(IV)]}{dt})_{Fe(III)+Mn(II)} = k_4[H^+]^a[Mn(II)][Fe(III)][S(IV)] \quad \text{(R3)}$$

$$-(\frac{d[S(IV)]}{dt})_{NO_2} = k_5[NO_{2(aq)}][S(IV)] \quad \text{(R4)}$$

where $k_0 = 2.4\times10^4$ M^{-1} s^{-1}, $k_1 = 3.7\times10^5$ M^{-1} s^{-1}, $k_2 = 1.5\times10^9$ M^{-1} s^{-1}, $k_3 = 7.45\times10^7$ M^{-1} s^{-1}, K = 13 M^{-1}, $k_4 = 3.72\times10^7$ M^{-1} s^{-1}, a = -0.74 (pH≤4.2) or $k_4 = 2.51\times10^{13}$ M^{-1} s^{-1}, a = 0.67 (pH>4.2), and

k_5 = (1.24-1.67)×10^7 M^{-1} s^{-1} (5.3≤pH≤8.7, the linear interpolated values were used for pH between 5.3 and 8.7) at 298 K (Clifton et al., 1988); [$O_{3(aq)}$], [$H_2O_{2(aq)}$] and [$NO_{2(aq)}$] could be calculated by the Henry's constants which are 1.1×10^{-2} M atm^{-1}, 1.0×10^5 M atm^{-1} and 1.0×10^{-2} M atm^{-1} at 298 K for O_3, H_2O_2 and NO_2 respectively (Seinfeld and Pandis, 2006). As for [Fe(III)] and [Mn(II)], their concentrations entirely depended on the values of pH due to the precipitation equilibriums of $Fe(OH)_3$ and $Mn(OH)_2$ (Graedel and Weschler, 1981). Considering the aqueous-phase ionization equilibrium of SO_2, the Henry's constants of HSO_3^-, SO_3^{2-} and S(IV) could be expressed by the equations as follows (Seinfeld and Pandis, 2006):

$$H^*_{HSO_3^-} = H_{SO_2}\frac{K_{S1}}{[H^+]} \quad \text{(R5)}$$

$$H^*_{SO_3^{2-}} = H_{SO_2}\frac{K_{S1}K_{S2}}{[H^+]^2} \quad \text{(R6)}$$

$$H^*_{S(IV)} = H_{SO_2}(1 + \frac{K_{S1}}{[H^+]} + \frac{K_{S1}K_{S2}}{[H^+]^2}) \quad \text{(R7)}$$

where H_{SO2} = 1.23 M atm^{-1}, K_{S1} = 1.3×10^{-2} M and K_{S2} = 6.6×10^{-8} M at 298 K. In addition, all of rate constants (k), Henry's constants (H) and ionization constants (K) are evidently influenced on the ambient temperature and are calibrated by the formulas as follows (Seinfeld and Pandis, 2006):

$$k(T) = k(T_0)e^{[-\frac{E}{R}(\frac{1}{T}-\frac{1}{T_0})]} \quad \text{(R8)}$$

$$H(T) = H(T_0)e^{[-\frac{\Delta H}{R}(\frac{1}{T}-\frac{1}{T_0})]} \quad \text{(R9)}$$

$$K(T) = K(T_0)e^{[-\frac{E}{R}(\frac{1}{T}-\frac{1}{T_0})]} \quad \text{(R10)}$$

where T is the ambient temperature, T_0=298 K, both E/R and ΔH/R varied in the different equations and their values could be found in Cheng et al., (2016).

Furthermore, mass transport was also considered for multiphase reactions in different medium and across the interface in section M3 of the SIs.

3. Results and Discussion

3.1. Variation characteristics of the species in $PM_{2.5}$ and typical gaseous pollutants

The concentrations of the species in $PM_{2.5}$ and typical gaseous pollutants including NO_2, SO_2, O_3, HONO and H_2O_2 as well as atmospheric RH are shown in Figure 1. The meteorological parameters (wind speed, wind direction, ambient temperature and direct radiation (DR)) as well as the concentrations of $PM_{2.5}$ are displayed in Figure S2. During the sampling period, the concentrations of the species in $PM_{2.5}$ and typical gaseous pollutants varied similarly on a timescale of hours with a distinct periodic cycle of 3-4 days, suggesting that meteorological conditions played a vital role in accumulation and dispersion of atmospheric pollutants (Xu et al., 2011;Zheng et al., 2015b). For example, the relatively high levels of $PM_{2.5}$ (>100 μg m^{-3}) usually occurred under the relatively stable meteorological conditions with the low south wind speed (<2 m s^{-1}) and the high RH (>60%) which favored the accumulation of pollutants. Besides meteorological conditions, the extremely high concentrations of the species in $PM_{2.5}$ might be mainly ascribed to strong emissions of primary pollutants and rapid formation of secondary aerosols during the wintertime in Beijing.

The average concentrations of the species in $PM_{2.5}$ and typical gaseous pollutants during clean or slightly polluted (C&SP) episodes ($PM_{2.5}$<75 μg m^{-3}), during polluted or heavy polluted (P&HP) episodes ($PM_{2.5}$≥75 μg m^{-3}) and during the whole sampling period are illustrated in Table 1. It is evident that the average concentrations of NO_3^-, SO_4^{2-}, NH_4^+, OC and EC during P&HP episodes were about a factor of 5.0, 4.1, 6.1, 3.6 and 3.2 greater than those during C&SP episodes, respectively, indicating that the formations of SIAs were more efficient compared to other species in $PM_{2.5}$ during the serious pollution episodes. Given that the average concentrations of gaseous

204 precursors (NO_2 and SO_2) during P&HP episodes were approximately a factor of 2.0-2.2 greater
205 than those during C&SP episodes, the obviously higher elevation of NO_3^- and SO_4^{2-} implied that
206 the oxidations of NO_2 and SO_2 by the major atmospheric oxidizing agents (OH radicals, O_3 and
207 H_2O_2 etc.) might be greatly accelerated due to the relatively high concentrations of oxidants and
208 atmospheric RH during the serious pollution episodes (Figure 1). The average concentration of
209 H_2O_2 was found to be a factor of 1.7 greater during P&HP episodes than during C&SP episodes,
210 indicating that atmospheric H_2O_2 might contribute to the formation of SIAs especially sulfate
211 during the serious pollution episodes with high atmospheric RH, which will be discussed in Sect.
212 3.3.2. However, the obvious decrease in O_3 average concentration was observed during P&HP
213 episodes compared to C&SP episodes, which was mainly attributed to the relatively weak solar
214 radiation and the titration of NO during the serious pollution episodes (Ye et al., 2018). In addition,
215 the evidently higher average concentration of HONO during P&HP episodes than during C&SP
216 episodes might be also due to the relatively weak solar radiation as well as the heterogeneous
217 reaction of NO_2 on particle surfaces during the serious pollution episodes (Tong et al., 2016;Wang
218 et al., 2017).

219 **3.2. Three serious pollution cases during the sampling period**

220 Based on the transition from the clean to polluted periods, three haze cases were identified
221 during the sampling period (Figure 1 and Figure S2): from 13:00 on January 8th to 1:00 on January
222 11th (Case 1), from 14:00 on January 14th to 7:00 on January 17th (Case 2), and from 8:00 on
223 January 19th to 2:00 on January 22nd (Case 3). The serious pollution duration in the three cases
224 could last 1-3 days due to the differences of their formation mechanisms.

225 In Case 1, the variation trends of the concentrations of the species in $PM_{2.5}$, NO_2, SO_2,

HONO and H_2O_2 were almost identical and exhibited three pollution peaks at night (Figure 1), which might be ascribed to the possibility that the decrease of nocturnal mixed boundary layer accelerated the pollutant accumulation (Bei et al., 2017;Zhong et al., 2019). Considering the relatively low RH (15-40%) and wind speeds (<2 m s^{-1}) in Case 1 (Figure S2), primary emissions around the sampling site were suspected to be a dominant source for the increase in the $PM_{2.5}$ concentrations. Further evidence is that the correlation between the concentrations of $PM_{2.5}$ and CO is better in Case 1 (R^2=0.55) than in Case 2 and Case 3 (R^2=0.20~0.52) (Figure S3). Identical to Case 1, three obvious pollution peaks were also observed in Case 2 (Figure 1). The variation trends of the concentrations of the species in $PM_{2.5}$ and typical gaseous pollutants at the first peak in Case 2 were found to be similar with those in Case 1, which were mainly attributed to their similar formation mechanism. However, the evident decreases in NO_x and SO_2 were observed when the concentrations of the species in $PM_{2.5}$ were increasing and the atmospheric oxidation pollutant (e.g. H_2O_2) concentration peaks were prior to others at the last two peaks in Case 2, suggesting that secondary formation from gaseous precursors might be dominant for $PM_{2.5}$ pollution. The relatively high RH (50-80%) and the low south wind speeds (<2 m s^{-1}) in Case 2 (Figure S2) provided further evidence for the above speculation. In contrast to Case 1 and Case 2, the relatively high south wind speeds (>3 m s^{-1}) (Figure S2) with the concentrations of the species in $PM_{2.5}$ and typical gaseous pollutants increasing slowly (Figure 1) at the beginning of Case 3 indicated that regional transportation might be responsible for the atmospheric species. Subsequently, the concentrations of the species in $PM_{2.5}$ remained relatively high when the atmospheric RH lasted more than 60%, implying that secondary formation from gaseous precursors dominated $PM_{2.5}$ pollution during the late period of Case 3.

The average mass proportions of the species in $PM_{2.5}$ in the three cases are illustrated in Figure S4, the proportions of the primary species such as EC (10-13%), Cl^- (6-7%) and Na^+ (4%) in the three cases were almost identical, indicating that primary particle emissions were relatively stable during the sampling period. However, the proportions of SIA in Case 2 (42%) and Case 3 (38%) were conspicuously greater than that in Case 1 (28%), further confirming that secondary formation of inorganic ions (e.g. nitrate, sulfate) made a significant contribution to atmospheric $PM_{2.5}$ in Case 2 and Case 3.

3.3. Formation mechanism of nitrate and sulfate during serious pollution episodes

As for nitrate and sulfate in the three cases, the highest mass proportion (18%) of nitrate was observed in Case 2, whereas the highest mass proportion (15%) of sulfate was found in Case 3 (Figure S4). Although the concentrations of SO_2 were obviously lower than the concentrations of NO_2 in both Case 2 and Case 3 (Figure 1 and Table 1), the extremely high proportion of sulfate in Case 3 might be ascribed to the long-lasting plateau of RH (Figure S2) because the aqueous-phase reaction could accelerate the conversion of SO_2 to SO_4^{2-}. To further investigate the pollution characteristics of nitrate and sulfate during the serious pollution episodes, the relations between NOR ($NOR = NO_3^- / (NO_3^-+NO_2)$) as well as SOR ($SOR = SO_4^{2-} / (SO_4^{2-}+SO_2)$) and RH are shown in Figure 2. There were obvious differences in the variations of NOR and SOR under different atmospheric RH conditions. The variation trends of NOR and SOR almost stayed the same when atmospheric RH was below 30%, and then simultaneously increased with atmospheric RH in the range of 30-60%. The enhanced gas-phase reaction and the heterogeneous reaction involving aerosol liquid water might make a remarkable contribution to the elevation of NOR and SOR, respectively, which were further discussed in the following section. Subsequently, the

variation trend of NOR slowly decreased whereas the variation trend of SOR significantly increased when atmospheric RH was above 60%, which was very similar with the previous studies (Sun et al., 2013;Zheng et al., 2015b). Considering that the heterogeneous reactions of NO_2 on particle surface were dependent on atmospheric RH due to the competition of water for surface reactive sites of particles (Ponczek et al., 2019), the slow reduction of NOR might be due to the suppressed heterogeneous reaction of NO_2 to nitrate formation under high RH condition (Tang et al., 2017), while the elevation of SOR revealed the dominant contribution of the aqueous-phase reaction to sulfate formation.

3.3.1. Formation mechanism of nitrate

Atmospheric nitrate is considered to be mainly from NO_2 oxidation by OH radical in the gas phase, heterogeneous uptake of NO_2 on the surface of particles and heterogeneous hydrolysis of N_2O_5 on wet aerosols or chloride-containing aerosols (He et al., 2014;He et al., 2018;Nie et al., 2014;Ravishankara, 1997;Wang et al., 2018b). Since atmospheric N_2O_5 is usually produced by the reaction of NO_3 radical with NO_2 as well as both NO_3 radical and N_2O_5 are easily photolytic during the daytime, the heterogeneous hydrolysis of N_2O_5 is a nighttime pathway for the formation of atmospheric nitrate (He et al., 2018;Wang et al., 2018b). As shown in Figure 3a, the mean values of NOR during the nighttime remarkably elevated with atmospheric RH increasing, the disproportionation of NO_2 and the heterogeneous hydrolysis of N_2O_5 involving aerosol liquid water were suspected to dominate the nocturnal formation of nitrate under high RH conditions during the sampling period (Ma et al., 2017;Wang et al., 2018b;Li et al., 2018). However, the productions of HONO and nitrate should be equal through the disproportionation of NO_2 (Ma et al., 2017), which could not explain the wide gaps between the average concentrations of HONO

(about 6.5 μg m^{-3}) and nitrate (about 20.1 μg m^{-3}) observed at the nighttime under high RH conditions during the sampling period. Thus, the disproportionation of NO_2 made insignificant contribution to the nocturnal formation of nitrate under high RH conditions. Considering that the formation of atmospheric NO_3 radical is mainly via the oxidation of NO_2 by O_3, the heterogeneous hydrolysis of N_2O_5 occurs only at high O_3 and NO_2 levels during the nighttime (He et al., 2018;Wang et al., 2018b). Therefore, the correlation between $[NO_2]^2 \times [O_3]$ and NOR can represent roughly the contribution of the heterogeneous hydrolysis of N_2O_5 to atmospheric nitrate at night. As shown in Figure 3b, the variations of $[NO_2]^2 \times [O_3]$ at the nighttime (18:00-7:00) were all positively correlated with NOR under the three different RH conditions, and their correlation under the RH ≥ 60% condition ($R^2 = 0.552$) was significantly stronger than those under the RH < 60% condition ($R^2 \leq 0.181$). It has been acknowledged that the correlation between two species means the impact of changes in one species on another. The stronger the correlation is, the greater the impact is. Therefore, the positive correlations between NOR and $[NO_2]^2 \times [O_3]$ indicated that the heterogeneous hydrolysis of N_2O_5 could contribute to the formation of atmospheric nitrate at the nighttime under different RH conditions. The significantly stronger correlations between NOR and $[NO_2]^2 \times [O_3]$ under the RH ≥ 60% condition than under the RH < 60% condition revealed that the heterogeneous hydrolysis of N_2O_5 made a remarkable contribution to atmospheric nitrate at the nighttime under high RH condition. Additionally, the obviously lower slope of the correlation between NOR and $[NO_2]^2 \times [O_3]$ under the RH ≥ 60% condition (slope = 11691) than under the RH < 60% condition (slope ≥ 17399) (Figure 3b) also suggested that the formation of atmospheric nitrate at the nighttime under high RH condition was more sensitive to the pathway of N_2O_5.

However, the obvious increase in the mean values of NOR during the daytime (especially for 10:00-17:00) under the 30%<RH<60% condition (Figure 3a) indicated that additional sources rather than the heterogeneous hydrolysis of N_2O_5 were responsible for the formation of nitrate. To explore the possible formation mechanisms of nitrate in this case, the daily variations of [Dust] (the sum of Ca^{2+} and Mg^{2+}) × [NO_2] and [HONO] (the main source of OH) × [DR] × [NO_2], which can represent roughly the heterogeneous reaction of NO_2 on the surface of mineral aerosols and the gas-phase reaction of NO_2 with OH, are shown in Figure 3c and Figure 3d, respectively. The mean values of [HONO] × [DR] × [NO_2] during the daytime were found to be remarkably greater under the 30%<RH<60% condition than under the RH≤30% condition, whereas the mean values of [Dust] × [NO_2] almost stayed the same under the two different RH conditions. Considering the coincident trend of NOR and [HONO] × [DR] × [NO_2] during the daytime (10:00-17:00) under the 30%<RH<60% condition, the gas-phase reaction of NO_2 with OH played a key role in the diurnal formation of nitrate at moderate RH levels with the haze pollution accumulating. It should be noted that the mean values of [HONO] × [DR] × [NO_2] decreased dramatically from 14:00 to 17:00 (Figure 3d), which was not responsible for the high mean values of NOR at that time (Figure 3a). However, the slight increase in the mean values of [Dust] × [NO_2] after 14:00 was observed under the 30%<RH<60% condition (Figure 3c) and hence the heterogeneous reaction of NO_2 on the surface of mineral aerosols was suspected to contribute to the diurnal formation of nitrate at that time under moderate RH condition.

3.3.2. Formation mechanism of sulfate

Atmospheric sulfate is principally from SO_2 oxidation pathway, including gas-phase reactions with OH radical or stabilized Criegee intermediates, heterogeneous-phase reactions on

the surface of particles and aqueous-phase reactions with dissolved O_3, NO_2, H_2O_2 and organic peroxides, as well as autoxidation catalyzed by TMI (Cheng et al., 2016;Li et al., 2018;Ravishankara, 1997;Shao et al., 2019;Wang et al., 2016;Xue et al., 2016;Zhang et al., 2018). As shown in Figure 4, similar to the daily variations of NOR, the mean values of SOR were found to elevated remarkably under the 30%<RH<60% condition compared to the RH≤30% condition, especially during 14:00-22:00, which might be mainly ascribed to the enhanced gas-phase reaction and the heterogeneous reaction of SO_2 involving aerosol liquid water under the relatively high RH condition. The extremely high mean values of SOR during the whole day under the RH≥60% condition implied that aqueous oxidation of SO_2 dominated the formation of sulfate during the severe pollution episodes, which was in line with previous studies (Zhang et al., 2018;Cheng et al., 2016). A key factor that influenced the aqueous oxidation pathways for sulfate formation has been considered to be the aerosol pH (Guo et al., 2017;Liu et al., 2017a), varying from 4.5 to 8.5 at different atmospheric RH and sulfate levels during the sampling period (Figure 5a) on the basis of the ISORROPIA-II model. Considering that the aqueous-phase chemistry of sulfate formation usually occurs in severe haze events with relatively high atmospheric RH, the aerosol pH (4.5-5.3) under the RH≥60% condition, which was lower than those (5.4-7.0) in the studies of Wang et al., (2016) and Cheng et al., (2016) but was slightly higher than those (3.0-4.9) in the studies of Liu et al., (2017a) and Guo et al., (2017), was adopted for evaluating sulfate production in this study. In addition, in terms of oxidants, the obvious increase in the average concentration of NO_2 (Figure 5b) and the evident decrease in the average concentration of O_3 (Figure 5d) were observed with the deterioration of $PM_{2.5}$ pollution. Furthermore, the average concentration of H_2O_2 was also found to be extremely high (0.25 ppb) under the HP condition (Figure 5c) and was above 1 order of

magnitude higher than that (0.01 ppb) assumed by Cheng et al., (2016), which probably resulted in the underestimation of the contribution of H_2O_2 to sulfate formation in the study of Cheng et al., (2016).

To further explore the contribution of H_2O_2 to sulfate production rate under the HP condition, the parameters measured in this study (Table 2) and the same approach that was adopted by Cheng et al., (2016) were used to calculate sulfate production. As shown in Figure 6, the relationships between different aqueous oxidation pathways and aerosol pH in this study were found to be very similar with those of Cheng et al., (2016). However, the contribution of H_2O_2 to sulfate production rate was about a factor of 17 faster in this study (about 1.16 μg m^{-3} h^{-1}) than in the study (about 6.95×10^{-2} μg m^{-3} h^{-1}) of Cheng et al., (2016), implying that the contribution of H_2O_2 to sulfate formation was largely neglected. Furthermore, considering the aerosol pH calculated under the HP condition during the sampling period, the oxidation pathway of NO_2 might play an insignificant role in sulfate production rate (8.96×10^{-2}-0.56 μg m^{-3} h^{-1}) and its importance proposed by the previous studies (1.74-10.85 μg m^{-3} h^{-1}) was not necessarily expected.

4. Conclusion

Based on the comprehensive analysis of the pollution levels, the variation characteristics and the formation mechanisms of the key species in $PM_{2.5}$ and the typical gaseous pollutants during the winter haze pollution periods in Beijing, three serious haze pollution cases were obtained during the sampling period and the SIAs formations especially nitrate and sulfate were found to make an evident contribution to atmospheric $PM_{2.5}$ under the relatively high RH condition. The significant correlation between $[NO_2]^2 \times [O_3]$ and NOR at night under the RH≥60% condition indicated that the heterogeneous hydrolysis of N_2O_5 on wet aerosols was responsible for the

nocturnal formation of nitrate under extremely high RH conditions. The more coincident trend of NOR and [HONO] × [DR] × [NO_2] than [Dust] × [NO_2] during the daytime under the 30%<RH<60% condition suggested that the gas-phase reaction of NO_2 with OH played a key role in the diurnal formation of nitrate under moderate RH conditions. The extremely high mean values of SOR during the whole day under the RH≥60% condition could be explained by the dominant contribution of aqueous-phase reaction of SO_2 to atmospheric sulfate formation during the severe pollution episodes. According to the parameters measured in this study and the same approach that was adopted by Cheng et al., (2016), the oxidation pathway of H_2O_2 rather than NO_2 was found to contribute greatly to atmospheric sulfate formation.

Our results revealed that the heavy pollution events in winter usually occurred with high concentration levels of pollutants and oxidants as well as high liquid water contents of moderately acidic aerosols in the NCP. Thus, emission controls of NO_x, SO_2 and VOCs especially under the extremely high RH conditions are expected to reduce largely the pollution levels of nitrate and sulfate in northern China and even in other pollution regions of China.

Data availability. Data are available from the corresponding author upon request (yjmu@rcees.ac.cn)

Author contributions. YJM designed the experiments. PFL carried out the experiments and prepared the manuscript. CY and CYX carried out the experiments. CLZ was involved in part of the work. XS provided the meteorological data and trace gases in Beijing.

Competing interests. The authors declare that they have no conflict of interest.

Acknowledgement. This work was supported by the National research program for Key issues in air pollution control (No. DQGG0103, DQGG0209, DQGG0206), the National Natural Science Foundation of China (No. 91544211, 4127805, 41575121, 21707151), the National Key Research and Development Program of China (No. 2016YFC0202200, 2017YFC0209703, 2017YFF0108301) and Key Laboratory of Atmospheric Chemistry, China Meteorological Administration (No. 2018B03).

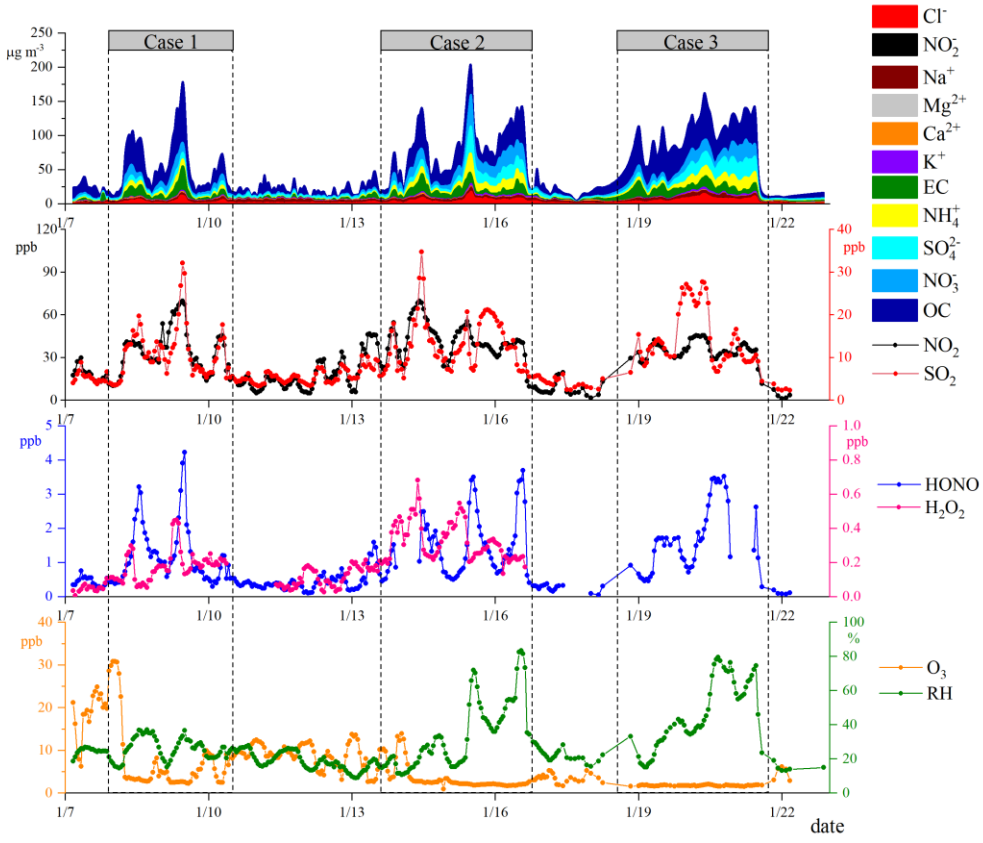

Figure 1. Time series of the species in $PM_{2.5}$ and typical gaseous pollutants (NO_2, SO_2, O_3, HONO and H_2O_2) as well as atmospheric RH during the sampling period.

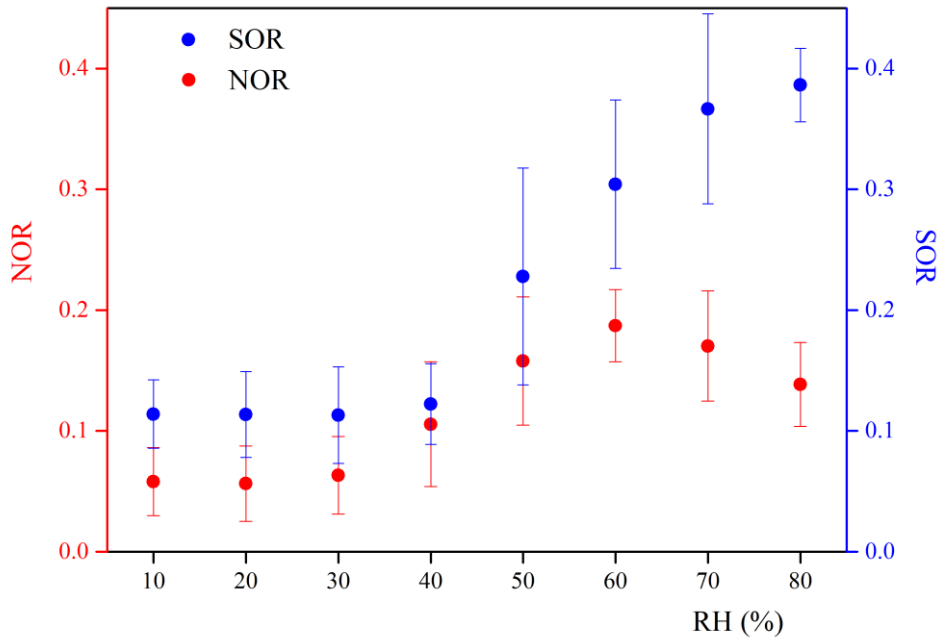

Figure 2. The relations between NOR as well as SOR and RH during the sampling period.

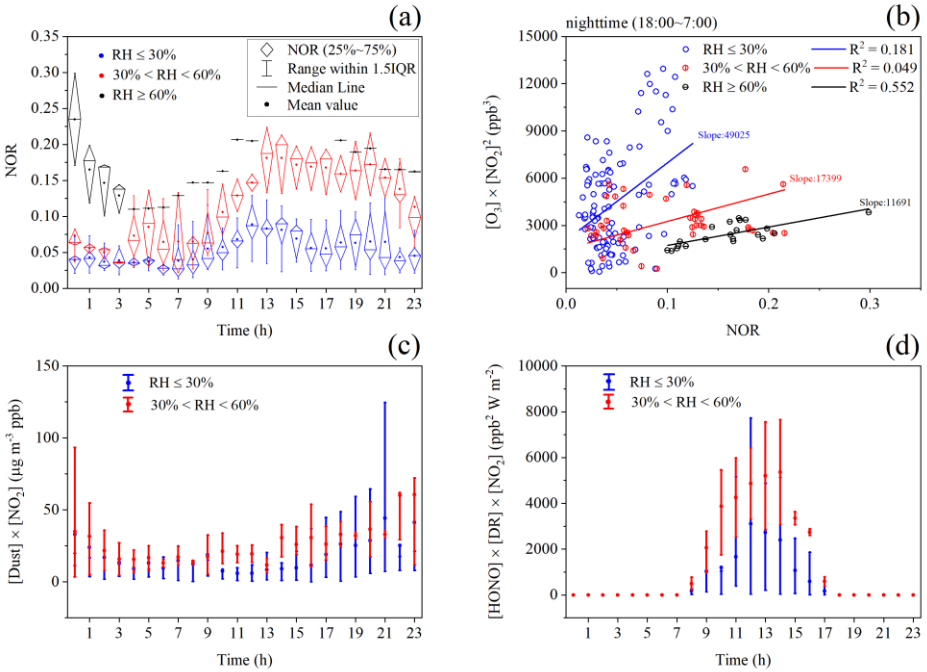

Figure 3. Daily variation of NOR (a), the correlation between NOR and $[NO_2]^2 \times [O_3]$ at the nighttime (18:00-7:00) (b), daily variations of [Dust] × $[NO_2]$ and [HONO] × [DR] × $[NO_2]$ (c, d) under different atmospheric RH conditions during the sampling period.

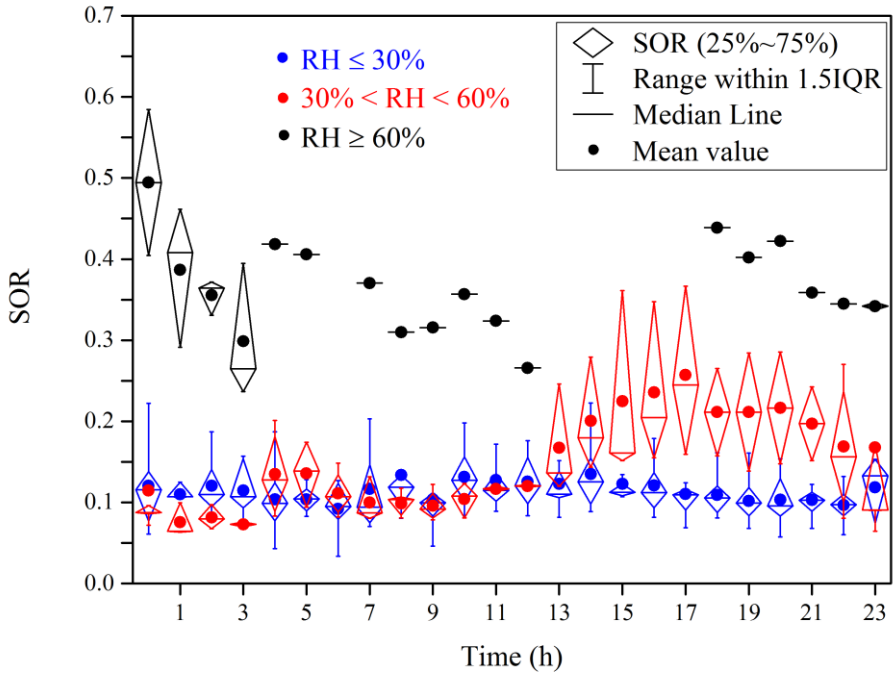

Figure 4. Daily variation of SOR under different atmospheric RH conditions during the sampling period.

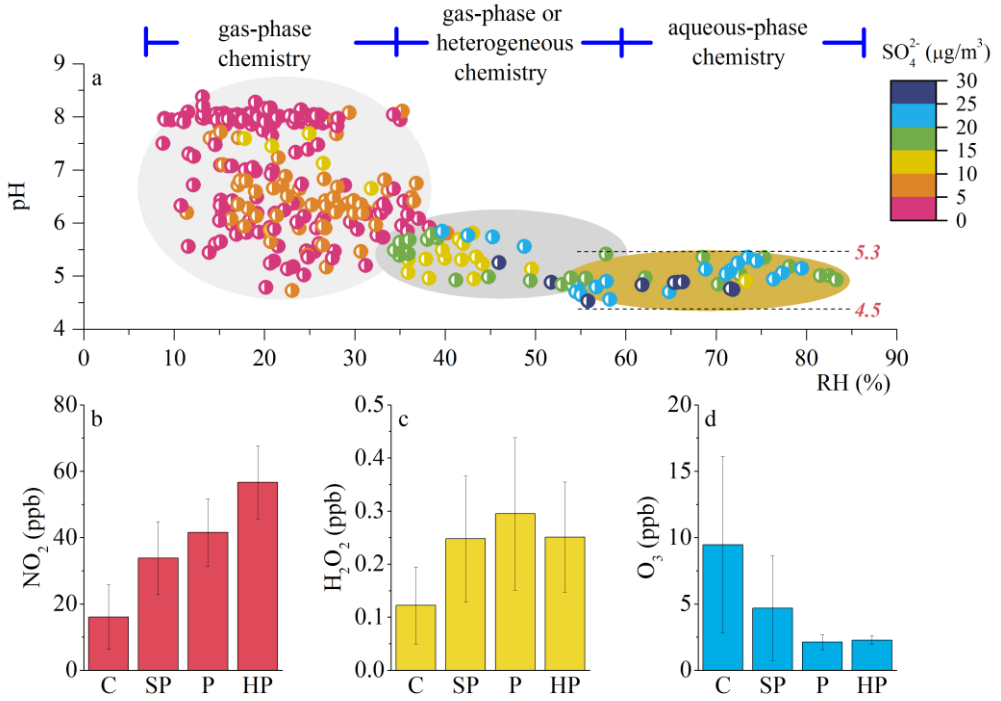

Figure 5. The correlations among aerosol pH, atmospheric RH and atmospheric SO_4^{2-} (a), the average concentrations of NO_2, H_2O_2 and O_3 (b, c, d) under different pollution conditions (clean (C), $PM_{2.5}$<35 μg m^{-3}; slightly polluted (SP), 35 μg m^{-3}<$PM_{2.5}$<75 μg m^{-3}; polluted (P), 75 μg

m^{-3}<$PM_{2.5}$<150 μg m^{-3}; heavy polluted (HP), $PM_{2.5}$>150 μg m^{-3}) during the sampling period.

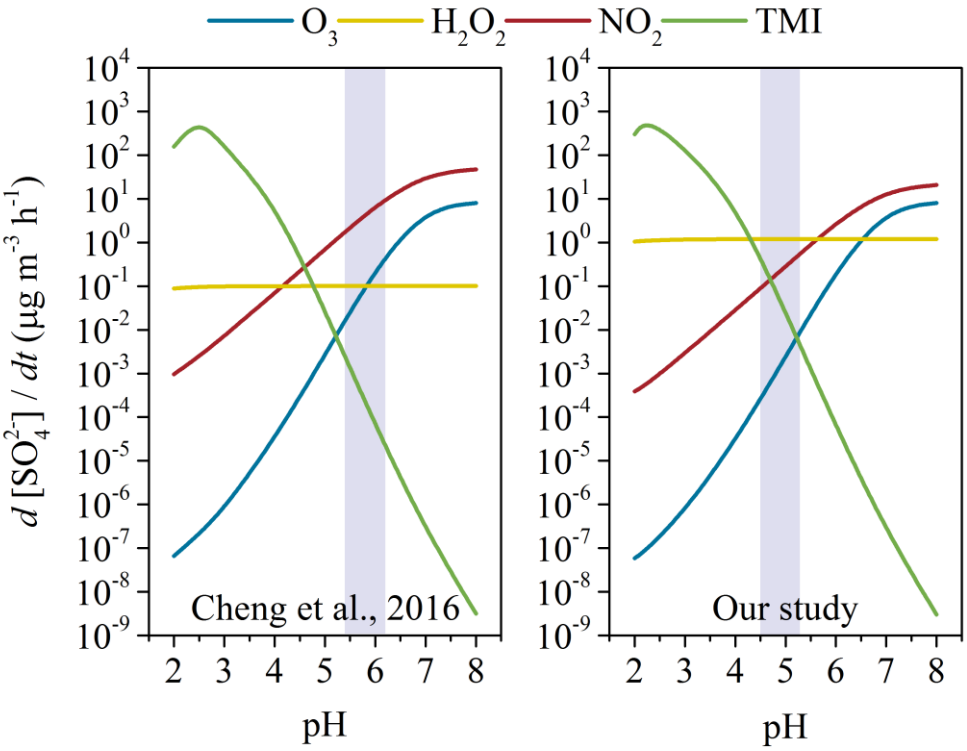

Figure 6. The comparison of aqueous-phase sulfate production by SO_2 oxidation under different aerosol pH conditions between in the study of Cheng et al., (2016) and in this study.

Table 1. The average concentrations of the species in $PM_{2.5}$ (μg m^{-3}) and typical gaseous pollutants (ppb) during C&SP episodes ($PM_{2.5}$<75 μg m^{-3}), during P&HP episodes ($PM_{2.5}$≥75 μg m^{-3}) and during the whole sampling period.

species	during C&SP episodes (n=210)	during P&HP episodes (n=108)	total (n=318)
$PM_{2.5}$	30.00 ± 17.79	113.35 ± 28.10	58.31 ± 45.15
Na^+	2.88 ± 1.11	3.68 ± 1.19	3.15 ± 1.21
Mg^{2+}	0.05 ± 0.03	0.08 ± 0.06	0.06 ± 0.04
Ca^{2+}	0.52 ± 0.33	0.67 ± 0.48	0.58 ± 0.40
K^+	0.81 ± 0.42	1.84 ± 0.73	1.16 ± 0.73
NH_4^+	1.90 ± 1.90	11.52 ± 4.93	5.17 ± 5.62
SO_4^{2-}	3.64 ± 1.87	14.96 ± 7.80	7.47 ± 7.18
NO_3^-	3.44 ± 3.57	17.15 ± 7.36	8.10 ± 8.32
Cl^-	1.89 ± 1.20	7.35 ± 2.97	3.73 ± 3.26
NO_2^-	0.06 ± 0.08	0.06 ± 0.05	0.06 ± 0.07
OC	12.10 ± 9.25	43.34 ± 13.88	22.73 ± 18.48
EC	3.98 ± 3.42	12.69 ± 6.43	7.58 ± 6.51
NO_x	39.38 ± 35.25	107.71 ± 58.44	62.59 ± 54.98
NO_2	21.46 ± 13.04	42.81 ± 10.96	28.71 ± 15.98
SO_2	6.99 ± 3.64	15.70 ± 6.55	9.95 ± 6.35

O_3	8.01 ± 6.35	2.13 ± 0.56	6.01 ± 5.87
HONO	0.60 ± 0.43	1.90 ± 0.97	1.01 ± 0.87
H_2O_2	0.17 ± 0.11	0.29 ± 0.14	0.20 ± 0.13

Table 2. The comparisons for parameters of sulfate production rate calculations between in the study of Cheng et al., (2016) and in this work during the most polluted haze periods

Parameters	This study	Cheng et al., (2016)
NO_2	57 ppb	66 ppb
H_2O_2	0.25 ppb	0.01 ppb
O_3	2 ppb	1 ppb
SO_2	35 ppb	40 ppb
Fe(III)[a]	18 ng m^{-3}	18 ng m^{-3}
Mn(II)[a]	42 ng m^{-3}	42 ng m^{-3}
ALWC	146 μg m^{-3}	300 μg m^{-3}
Aerosol droplet radius (R)[a]	0.15 μm	0.15 μm
Temperature	270 K	271 K
pH	4.5-5.3	5.4-6.2

[a]: both the concentrations of Fe(III) and Mn(II) and aerosol droplet radius were not measured in this study and were derived from Cheng et al., (2016).

References

Bei, N., Wu, J., Elser, M., Feng, T., Cao, J., El-Haddad, I., Li, X., Huang, R., Li, Z., Long, X., Xing, L., Zhao, S., Tie, X., Prévôt, A. S. H., and Li, G.: Impacts of meteorological uncertainties on the haze formation in Beijing–Tianjin–Hebei (BTH) during wintertime: a case study, Atmospheric Chemistry and Physics, 17, 14579-14591, 10.5194/acp-17-14579-2017, 2017.

Bougiatioti, A., Nikolaou, P., Stavroulas, I., Kouvarakis, G., Weber, R., Nenes, A., Kanakidou, M., and Mihalopoulos, N.: Particle water and pH in the eastern Mediterranean: source variability and implications for nutrient availability, Atmospheric Chemistry and Physics, 16, 4579-4591, 10.5194/acp-16-4579-2016, 2016.

Chan, C. K., and Yao, X.: Air pollution in mega cities in China, Atmospheric Environment, 42, 1-42, 10.1016/j.atmosenv.2007.09.003, 2008.

Chen, L. H., Sun, Y. Y., Wu, X. C., Zhang, Y. X., Zheng, C. H., Gao, X., and Cen, K.: Unit-based emission inventory and uncertainty assessment of coal-fired power plants, Atmospheric Environment, 99, 527-535, 10.1016/j.atmosenv.2014.10.023, 2014.

Cheng, Y., Zheng, G., Wei, C., Mu, Q., Zheng, B., Wang, Z., Gao, M., Zhang, Q., He, K., Carmichael, G., Pöschl, U., and Su, H.: Reactive nitrogen chemistry in aerosol water as a source of sulfate during haze events in China, Science Advances, 2, 1-11, 10.1126/sciadv.1601530, 2016.

Clifton, C. L., Altstein, N., and Huie, R. E.: Rate-constant for the reaction of NO_2 with sulfur(IV) over the pH range 5.3-13, Environ. Sci. Technol., 22, 586-589, 10.1021/es00170a018, 1988.

Dai, Q., Bi, X., Song, W., Li, T., Liu, B., Ding, J., Xu, J., Song, C., Yang, N., Schulze, B. C., Zhang, Y., Feng, Y., and Hopke, P. K.: Residential coal combustion as a source of primary sulfate in Xi'an, China, Atmospheric Environment, 196, 66-76, 10.1016/j.atmosenv.2018.10.002, 2019.

Ding, J., Zhao, P., Su, J., Dong, Q., Du, X., and Zhang, Y.: Aerosol pH and its driving factors in Beijing,

Atmospheric Chemistry and Physics, 19, 7939-7954, 10.5194/acp-19-7939-2019, 2019.
Du, Q., Zhang, C., Mu, Y., Cheng, Y., Zhang, Y., Liu, C., Song, M., Tian, D., Liu, P., Liu, J., Xue, C., and Ye, C.: An important missing source of atmospheric carbonyl sulfide: Domestic coal combustion, Geophysical Research Letters, 43, 8720-8727, 10.1002/2016gl070075, 2016.
Fountoukis, C., and Nenes, A.: ISORROPIA II: a computationally efficient thermodynamic equilibrium model for K^+-Ca^{2+}-Mg^{2+}-NH_4^+-Na^+-SO_4^{2-}-NO_3^--Cl^--H_2O aerosols, Atmospheric Chemistry and Physics, 7, 4639-4659, 2007.
Ge, X., He, Y., Sun, Y., Xu, J., Wang, J., Shen, Y., and Chen, M.: Characteristics and Formation Mechanisms of Fine Particulate Nitrate in Typical Urban Areas in China, Atmosphere, 8, 62, 10.3390/atmos8030062, 2017.
Graedel, T. E., and Weschler, C. J.: Chemistry within aqueous atmospheric aerosols and raindrops, Reviews of Geophysics, 19, 505-539, 10.1029/RG019i004p00505, 1981.
Guo, H., Xu, L., Bougiatioti, A., Cerully, K. M., Capps, S. L., Hite, J. R., Carlton, A. G., Lee, S. H., Bergin, M. H., Ng, N. L., Nenes, A., and Weber, R. J.: Fine-particle water and pH in the southeastern United States, Atmospheric Chemistry and Physics, 15, 5211-5228, 10.5194/acp-15-5211-2015, 2015.
Guo, H., Weber, R. J., and Nenes, A.: High levels of ammonia do not raise fine particle pH sufficiently to yield nitrogen oxide-dominated sulfate production, Scientific reports, 7, 12109, 10.1038/s41598-017-11704-0, 2017.
Guo, S., Hu, M., Zamora, M. L., Peng, J., Shang, D., Zheng, J., Du, Z., Wu, Z., Shao, M., Zeng, L., Molina, M. J., and Zhang, R.: Elucidating severe urban haze formation in China, Proceedings of the National Academy of Sciences of the United States of America, 111, 17373-17378, 10.1073/pnas.1419604111, 2014.
He, H., Wang, Y., Ma, Q., Ma, J., Chu, B., Ji, D., Tang, G., Liu, C., Zhang, H., and Hao, J.: Mineral dust and NO_x promote the conversion of SO_2 to sulfate in heavy pollution days, Scientific reports, 4, 1-5, 10.1038/srep04172, 2014.
He, P., Xie, Z., Chi, X., Yu, X., Fan, S., Kang, H., Liu, C., and Zhan, H.: Atmospheric $\Delta 17O(NO_3^-)$ reveals nocturnal chemistry dominates nitrate production in Beijing haze, Atmospheric Chemistry and Physics, 18, 14465-14476, 10.5194/acp-18-14465-2018, 2018.
Hennigan, C. J., Izumi, J., Sullivan, A. P., Weber, R. J., and Nenes, A.: A critical evaluation of proxy methods used to estimate the acidity of atmospheric particles, Atmospheric Chemistry and Physics, 15, 2775-2790, 10.5194/acp-15-2775-2015, 2015.
Huang, R. J., Zhang, Y., Bozzetti, C., Ho, K. F., Cao, J. J., Han, Y., Daellenbach, K. R., Slowik, J. G., Platt, S. M., Canonaco, F., Zotter, P., Wolf, R., Pieber, S. M., Bruns, E. A., Crippa, M., Ciarelli, G., Piazzalunga, A., Schwikowski, M., Abbaszade, G., Schnelle-Kreis, J., Zimmermann, R., An, Z., Szidat, S., Baltensperger, U., El Haddad, I., and Prevot, A. S.: High secondary aerosol contribution to particulate pollution during haze events in China, Nature, 514, 218-222, 10.1038/nature13774, 2014.
Ibusuki, T., and Takeuchi, K.: Sulfur-dioxide oxidation by oxygen catalyzed by mixtures of manganese(II) and iron(III) in aqueous-solutions at environmental reaction conditions, Atmospheric Environment, 21, 1555-1560, 10.1016/0004-6981(87)90317-9, 1987.
Li, G., Bei, N., Cao, J., Huang, R., Wu, J., Feng, T., Wang, Y., Liu, S., Zhang, Q., Tie, X., and Molina, L. T.: A possible pathway for rapid growth of sulfate during haze days in China, Atmospheric Chemistry and Physics, 17, 3301-3316, 10.5194/acp-17-3301-2017, 2017.
Li, J., Liao, H., Hu, J., and Li, N.: Severe particulate pollution days in China during 2013-2018 and the associated typical weather patterns in Beijing-Tianjin-Hebei and the Yangtze River Delta regions,

513 Environ Pollut, 248, 74-81, 10.1016/j.envpol.2019.01.124, 2019.
514 Li, L., Hoffmann, M. R., and Colussi, A. J.: Role of nitrogen dioxide in the production of sulfate during
515 Chinese haze-aerosol episodes, Environ Sci Technol, 52, 2686-2693, 10.1021/acs.est.7b05222, 2018.
516 Li, Q., Li, X., Jiang, J., Duan, L., Ge, S., Zhang, Q., Deng, J., Wang, S., and Hao, J.: Semi-coke
517 briquettes: towards reducing emissions of primary $PM_{2.5}$, particulate carbon, and carbon monoxide
518 from household coal combustion in China, Scientific reports, 6, 1-10, 10.1038/srep19306, 2016.
519 Liu, M., Song, Y., Zhou, T., Xu, Z., Yan, C., Zheng, M., Wu, Z., Hu, M., Wu, Y., and Zhu, T.: Fine
520 particle pH during severe haze episodes in northern China, Geophysical Research Letters, 44, 1-9,
521 10.1002/2017GL073210, 2017a.
522 Liu, P., Zhang, C., Mu, Y., Liu, C., Xue, C., Ye, C., Liu, J., Zhang, Y., and Zhang, H.: The possible
523 contribution of the periodic emissions from farmers' activities in the North China Plain to atmospheric
524 water-soluble ions in Beijing, Atmospheric Chemistry and Physics, 16, 10097-10109,
525 10.5194/acp-16-10097-2016, 2016.
526 Liu, P., Zhang, C., Xue, C., Mu, Y., Liu, J., Zhang, Y., Tian, D., Ye, C., Zhang, H., and Guan, J.: The
527 contribution of residential coal combustion to atmospheric $PM_{2.5}$ in northern China during winter,
528 Atmospheric Chemistry and Physics, 17, 11503-11520, 10.5194/acp-17-11503-2017, 2017b.
529 Ma, Q., Wang, T., Liu, C., He, H., Wang, Z., Wang, W., and Liang, Y.: SO_2 Initiates the efficient
530 conversion of NO_2 to HONO on MgO Surface, Environ Sci Technol, 51, 3767-3775,
531 10.1021/acs.est.6b05724, 2017.
532 Meng, Z. Y., Lin, W. L., Jiang, X. M., Yan, P., Wang, Y., Zhang, Y. M., Jia, X. F., and Yu, X. L.:
533 Characteristics of atmospheric ammonia over Beijing, China, Atmospheric Chemistry and Physics, 11,
534 6139-6151, 10.5194/acp-11-6139-2011, 2011.
535 Murphy, J. G., Gregoire, P. K., Tevlin, A. G., Wentworth, G. R., Ellis, R. A., Markovic, M. Z., and
536 VandenBoer, T. C.: Observational constraints on particle acidity using measurements and modelling of
537 particles and gases, Faraday Discussions, 200, 379-395, 10.1039/c7fd00086c, 2017.
538 Nie, W., Ding, A., Wang, T., Kerminen, V. M., George, C., Xue, L., Wang, W., Zhang, Q., Petaja, T., Qi,
539 X., Gao, X., Wang, X., Yang, X., Fu, C., and Kulmala, M.: Polluted dust promotes new particle
540 formation and growth, Scientific reports, 4, 1-6, 10.1038/srep06634, 2014.
541 Pathak, R. K., Louie, P. K. K., and Chan, C. K.: Characteristics of aerosol acidity in Hong kong,
542 Atmospheric Environment, 38, 2965-2974, 10.1016/j.atmosenv.2004.02.044, 2004.
543 Ponczek, M., Hayeck, N., Emmelin, C., and George, C.: Heterogeneous photochemistry of dicarboxylic
544 acids on mineral dust, Atmospheric Environment, 212, 262-271, 10.1016/j.atmosenv.2019.05.032,
545 2019.
546 Quan, J., Tie, X., Zhang, Q., Liu, Q., Li, X., Gao, Y., and Zhao, D.: Characteristics of heavy aerosol
547 pollution during the 2012–2013 winter in Beijing, China, Atmospheric Environment, 88, 83-89,
548 10.1016/j.atmosenv.2014.01.058, 2014.
549 Ravishankara, A.: Heterogeneous and multiphase chemistry in the troposphere, Science, 276,
550 1058-1065, 1997.
551 Seinfeld, J. H., and Pandis, S. N.: Atmospheric Chemistry and Physics, from Air Pollution to Climate
552 Change, Wiley, 429-443 pp., 2006.
553 Shao, J., Chen, Q., Wang, Y., Lu, X., He, P., Sun, Y., Shah, V., Martin, R. V., Philip, S., Song, S., Zhao,
554 Y., Xie, Z., Zhang, L., and Alexander, B.: Heterogeneous sulfate aerosol formation mechanisms during
555 wintertime Chinese haze events: air quality model assessment using observations of sulfate oxygen
556 isotopes in Beijing, Atmospheric Chemistry and Physics, 19, 6107-6123, 10.5194/acp-19-6107-2019,

2019.
Shi, G., Xu, J., Peng, X., Xiao, Z., Chen, K., Tian, Y., Guan, X., Feng, Y., Yu, H., Nenes, A., and Russell, A. G.: pH of aerosols in a polluted atmosphere: source contributions to highly acidic aerosol, Environ Sci Technol, 51, 4289-4296, 10.1021/acs.est.6b05736, 2017.
Sun, Y., Wang, Z., Fu, P., Jiang, Q., Yang, T., Li, J., and Ge, X.: The impact of relative humidity on aerosol composition and evolution processes during wintertime in Beijing, China, Atmospheric Environment, 77, 927-934, 10.1016/j.atmosenv.2013.06.019, 2013.
Tang, M., Huang, X., Lu, K., Ge, M., Li, Y., Cheng, P., Zhu, T., Ding, A., Zhang, Y., Gligorovski, S., Song, W., Ding, X., Bi, X., and Wang, X.: Heterogeneous reactions of mineral dust aerosol: implications for tropospheric oxidation capacity, Atmospheric Chemistry and Physics, 17, 11727-11777, 10.5194/acp-17-11727-2017, 2017.
Tham, Y. J., Wang, Z., Li, Q., Wang, W., Wang, X., Lu, K., Ma, N., Yan, C., Kecorius, S., Wiedensohler, A., Zhang, Y., and Wang, T.: Heterogeneous N_2O_5 uptake coefficient and production yield of $ClNO_2$ in polluted northern China: roles of aerosol water content and chemical composition, Atmospheric Chemistry and Physics, 18, 13155-13171, 10.5194/acp-18-13155-2018, 2018.
Tong, S. R., Hou, S. Q., Zhang, Y., Chu, B. W., Liu, Y. C., He, H., Zhao, P. S., and Ge, M. F.: Exploring the nitrous acid (HONO) formation mechanism in winter Beijing: direct emissions and heterogeneous production in urban and suburban areas, Faraday Discussions, 189, 213-230, 10.1039/c5fd00163c, 2016.
Wang, G., Zhang, R., Gomez, M. E., Yang, L., Levy Zamora, M., Hu, M., Lin, Y., Peng, J., Guo, S., Meng, J., Li, J., Cheng, C., Hu, T., Ren, Y., Wang, Y., Gao, J., Cao, J., An, Z., Zhou, W., Li, G., Wang, J., Tian, P., Marrero-Ortiz, W., Secrest, J., Du, Z., Zheng, J., Shang, D., Zeng, L., Shao, M., Wang, W., Huang, Y., Wang, Y., Zhu, Y., Li, Y., Hu, J., Pan, B., Cai, L., Cheng, Y., Ji, Y., Zhang, F., Rosenfeld, D., Liss, P. S., Duce, R. A., Kolb, C. E., and Molina, M. J.: Persistent sulfate formation from London Fog to Chinese haze, Proceedings of the National Academy of Sciences of the United States of America, 113, 13630-13635, 2016.
Wang, G., Zhang, F., Peng, J., Duan, L., Ji, Y., Marrero-Ortiz, W., Wang, J., Li, J., Wu, C., Cao, C., Wang, Y., Zheng, J., Secrest, J., Li, Y., Wang, Y., Li, H., Li, N., and Zhang, R.: Particle acidity and sulfate production during severe haze events in China cannot be reliably inferred by assuming a mixture of inorganic salts, Atmospheric Chemistry and Physics, 18, 10123-10132, 10.5194/acp-18-10123-2018, 2018a.
Wang, H., Lu, K., Chen, X., Zhu, Q., Wu, Z., Wu, Y., and Sun, K.: Fast particulate nitrate formation via N_2O_5 uptake aloft in winter in Beijing, Atmospheric Chemistry and Physics, 18, 10483-10495, 10.5194/acp-18-10483-2018, 2018b.
Wang, H., Lu, K., Guo, S., Wu, Z., Shang, D., Tan, Z., Wang, Y., Le Breton, M., Lou, S., Tang, M., Wu, Y., Zhu, W., Zheng, J., Zeng, L., Hallquist, M., Hu, M., and Zhang, Y.: Efficient N_2O_5 uptake and NO_3 oxidation in the outflow of urban Beijing, Atmospheric Chemistry and Physics, 18, 9705-9721, 10.5194/acp-18-9705-2018, 2018c.
Wang, J., Zhang, X., Guo, J., Wang, Z., and Zhang, M.: Observation of nitrous acid (HONO) in Beijing, China: Seasonal variation, nocturnal formation and daytime budget, The Science of the total environment, 587-588, 350-359, 10.1016/j.scitotenv.2017.02.159, 2017.
Wang, Y., Yao, L., Wang, L., Liu, Z., Ji, D., Tang, G., Zhang, J., Sun, Y., Hu, B., and Xin, J.: Mechanism for the formation of the January 2013 heavy haze pollution episode over central and eastern China, Science China Earth Sciences, 57, 14-25, 10.1007/s11430-013-4773-4, 2013.

Weber, R. J., Guo, H., Russell, A. G., and Nenes, A.: High aerosol acidity despite declining atmospheric sulfate concentrations over the past 15 years, Nature Geoscience, 9, 282-285, 10.1038/ngeo2665, 2016.

Wu, J., Bei, N., Hu, B., Liu, S., Zhou, M., Wang, Q., Li, X., Liu, L., Feng, T., Liu, Z., Wang, Y., Cao, J., Tie, X., Wang, J., Molina, L. T., and Li, G.: Is water vapor a key player of the wintertime haze in North China Plain?, Atmospheric Chemistry and Physics, 19, 8721-8739, 10.5194/acp-19-8721-2019, 2019.

Xu, L., Duan, F., He, K., Ma, Y., Zhu, L., Zheng, Y., Huang, T., Kimoto, T., Ma, T., Li, H., Ye, S., Yang, S., Sun, Z., and Xu, B.: Characteristics of the secondary water-soluble ions in a typical autumn haze in Beijing, Environ Pollut, 227, 296-305, 10.1016/j.envpol.2017.04.076, 2017.

Xu, W. Y., Zhao, C. S., Ran, L., Deng, Z. Z., Liu, P. F., Ma, N., Lin, W. L., Xu, X. B., Yan, P., He, X., Yu, J., Liang, W. D., and Chen, L. L.: Characteristics of pollutants and their correlation to meteorological conditions at a suburban site in the North China Plain, Atmospheric Chemistry and Physics, 11, 4353-4369, 10.5194/acp-11-4353-2011, 2011.

Xue, C., Ye, C., Ma, Z., Liu, P., Zhang, Y., Zhang, C., Tang, K., Zhang, W., Zhao, X., Wang, Y., Song, M., Liu, J., Duan, J., Qin, M., Tong, S., Ge, M., and Mu, Y.: Development of stripping coil-ion chromatograph method and intercomparison with CEAS and LOPAP to measure atmospheric HONO, The Science of the total environment, 646, 187-195, 10.1016/j.scitotenv.2018.07.244, 2019a.

Xue, C., Ye, C., Zhang, Y., Ma, Z., Liu, P., Zhang, C., Zhao, X., Liu, J., and Mu, Y.: Development and application of a twin open-top chambers method to measure soil HONO emission in the North China Plain, Sci. Total Environ., 659, 621-631, 10.1016/j.scitotenv.2018.12.245, 2019b.

Xue, J., Yuan, Z., Griffith, S. M., Yu, X., Lau, A. K., and Yu, J. Z.: Sulfate Formation Enhanced by a Cocktail of High NO_x, SO_2, Particulate Matter, and Droplet pH during Haze-Fog Events in Megacities in China: An Observation-Based Modeling Investigation, Environ Sci Technol, 50, 7325-7334, 10.1021/acs.est.6b00768, 2016.

Yang, T., Sun, Y., Zhang, W., Wang, Z., Liu, X., Fu, P., and Wang, X.: Evolutionary processes and sources of high-nitrate haze episodes over Beijing, Spring, J Environ Sci (China), 54, 142-151, 10.1016/j.jes.2016.04.024, 2017.

Yang, Y. R., Liu, X. G., Qu, Y., An, J. L., Jiang, R., Zhang, Y. H., Sun, Y. L., Wu, Z. J., Zhang, F., Xu, W. Q., and Ma, Q. X.: Characteristics and formation mechanism of continuous hazes in China: a case study during the autumn of 2014 in the North China Plain, Atmospheric Chemistry and Physics, 15, 8165-8178, 10.5194/acp-15-8165-2015, 2015.

Ye, C., Liu, P., Ma, Z., Xue, C., Zhang, C., Zhang, Y., Liu, J., Liu, C., Sun, X., and Mu, Y.: High H_2O_2 Concentrations Observed during Haze Periods during the Winter in Beijing: Importance of H_2O_2 Oxidation in Sulfate Formation, Environmental Science & Technology Letters, 5, 757-763, 10.1021/acs.estlett.8b00579, 2018.

Zhang, H., Chen, S., Zhong, J., Zhang, S., Zhang, Y., Zhang, X., Li, Z., and Zeng, X. C.: Formation of aqueous-phase sulfate during the haze period in China: Kinetics and atmospheric implications, Atmospheric Environment, 177, 93-99, 10.1016/j.atmosenv.2018.01.017, 2018.

Zhang, Q., He, K. B., and Huo, H.: Cleaning China's air, Nature, 484, 161-162, 2012.

Zhang, R., Wang, G., Guo, S., Zamora, M. L., Ying, Q., Lin, Y., Wang, W., Hu, M., and Wang, Y.: Formation of urban fine particulate matter, Chem Rev, 115, 3803-3855, 10.1021/acs.chemrev.5b00067, 2015.

Zhao, M., Wang, S., Tan, J., Hua, Y., Wu, D., and Hao, J.: Variation of Urban Atmospheric Ammonia Pollution and its Relation with PM2.5 Chemical Property in Winter of Beijing, China, Aerosol and Air

Quality Research, 16, 1390-1402, 10.4209/aaqr.2015.12.0699, 2016.
Zheng, B., Zhang, Q., Zhang, Y., He, K. B., Wang, K., Zheng, G. J., Duan, F. K., Ma, Y. L., and Kimoto, T.: Heterogeneous chemistry: a mechanism missing in current models to explain secondary inorganic aerosol formation during the January 2013 haze episode in North China, Atmospheric Chemistry and Physics, 15, 2031-2049, 10.5194/acp-15-2031-2015, 2015a.
Zheng, G. J., Duan, F. K., Su, H., Ma, Y. L., Cheng, Y., Zheng, B., Zhang, Q., Huang, T., Kimoto, T., Chang, D., Pöschl, U., Cheng, Y. F., and He, K. B.: Exploring the severe winter haze in Beijing: the impact of synoptic weather, regional transport and heterogeneous reactions, Atmospheric Chemistry and Physics, 15, 2969-2983, 10.5194/acp-15-2969-2015, 2015b.
Zhong, J., Zhang, X., Wang, Y., Wang, J., Shen, X., Zhang, H., Wang, T., Xie, Z., Liu, C., Zhang, H., Zhao, T., Sun, J., Fan, S., Gao, Z., Li, Y., and Wang, L.: The two-way feedback mechanism between unfavorable meteorological conditions and cumulative aerosol pollution in various haze regions of China, Atmospheric Chemistry and Physics, 19, 3287-3306, 10.5194/acp-19-3287-2019, 2019.